Supplemental information
Human bone perivascular niche-on-a-chip for studying metastatic colonization; Marturano-Kruik et al

Methods

Drugs and chemicals. Dulbecco's modified eagle medium (DMEM), penicillin-streptomycin solution (100×), trypsin/ethylenediaminetetraacetic acid (EDTA; 0.25%), basic fibroblast growth factor (bFGF) were purchased from Life Technologies. HyClone fetal bovine serum (FBS), Tris buffer, proteinase K, PBS, and CitriSolv were purchased from Fisher Scientific. Sunitinib was purchased from Cell Signaling.

Cell culture. Human mesenchymal stem cells (MSCs) were isolated from fresh bone marrow aspirates (Cambrex) by their attachment to the plastic surface - as previously described (1). Cells were expanded to the third passage in high glucose DMEM supplemented with 10% FBS, 1% penicillin–streptomycin, and 0.1 ng ml^{-1} bFGF. Human umbilical vein endothelial cells expressing red fluorescent protein (HUVECS/RFP) were expanded in endothelial growth medium (EGM-2 BulletKit media; Lonza). Breast cancer cells expressing green fluorescent protein - MDA-MB-231/GFP - or firefly luciferase gene - MDA-MB-231/Luc - (Cell Biolabs) were maintained in Dulbecco's modified Eagle's medium (Life Technologies) supplemented with 10% fetal bovine serum, 1% penicillin–streptomycin. All cell cultures were kept in a humidified incubator at 37°C and 5% CO_2.

3D bone matrix preparation and decellularization. Calve metacarpal joints (Green Village Packing) were cut into axial sections approximately 2 mm thick on a vertical bandsaw. Sections were selected based on approximate pore size of 0.5 mm from a region within the condyles. In order to convert the section into our desired scaffold geometry, it was cleaned under high-pressure streamed water, dried, and fixtured in a 3 axis CNC milling machine. The bone was machined with a standard 2 flute endmill to a final geometry of 6mm x 3mm x 1mm (length x depth x thickness). To remove cellular material, the scaffolds were washed with EDTA (0.1%) in PBS, EDTA (0.1%) in Tris (10 mM), and SDS (0.5%) in Tris (10 mM), followed by treatment with a solution of DNase and RNase in Tris buffer (10 mM). Decellularized bone scaffolds were thoroughly rinsed in deionized H_2O and freeze-dried. The scaffolds within the density range of 0.37–0.45 mg mm^{-3} where sterilized in ethanol (70% vol/vol), and conditioned in EGM2 overnight before cell seeding**.** To demonstrate the effectiveness of the decellularization protocol, DNA content of the bone before (native) and after decellularization was quantified using Quant-iT™ PicoGreen™ dsDNA Assay Kit (ThermoFisher) following the manufacturer's protocol and as previously described (2). Bone samples were digested at 60 °C over-night, the supernatant was collected and diluted as needed to a concentration within the linear range of the assay. A standard curve was used to convert fluorescence to total DNA. Samples were read using a fluorescent plate reader at an excitation wavelength of 480nm and an emission wavelength of 528 nm.

3D and 2D niche cultures. Bone marrow-derived stem cells were seeded alone, or with endothelial cells (HUVEC/RFP) at a 5:1 ratio to generate the perivascular niches. For the 3D culture, the bone matrix or a commercially available 3D polystyrene scaffold (3D Biotek) were used. Cells were suspended in EGM-2 (endothelial medium) at a concentration of $1x10^6$ cells in 20 µl. After depositing 10 µl of cellular suspension per scaffold, the plates were left undisturbed in a humidified incubator at 37°C and 5% CO_2 for 45 minutes to allow even cell seeding. This operation was repeated after flipping the scaffolds 180°. Then, samples were placed in an ultralow attachment 24-well plate (Sigma Aldrich) containing 1 ml of EGM-2. After 6 days, MDA-MB-231/GFP or MDA-MB-231/Luc cells ($25x10^3$ cells ml^{-1}) were suspended in DMEM with 1% fetal bovine serum and 1% penicillin–streptomycin (serum reduced medium). Cancer cells were seeded (10 µl $scaffold^{-1}$) after washing scaffolds thrice with PBS. Cells were allowed to settle for 30 minutes at room temperature. Additional 10 µl of cells suspension was added after flipping the scaffolds 180°, for a total of 20 µl $scaffold^{-1}$. Tissues were placed in an

ultralow-attachment 24-well plate containing 1 ml of cancer medium. Plates were kept for 24 hours in a humidified incubator at 37°C and 5% CO_2. At day 7 samples were either kept statically in the tissue culture plates or placed in the microfluidic chip and cultured for additional 7 days. Culture medium was replaced three times a week. For monolayer cultures, bone marrow-derived stem cells were suspended in 0.2 µl of EGM-2 (endothelial medium) and seeded alone at a density of $30x10^3$ cells $well^{-1}$ on 96 well-plate, or with endothelial cells (HUVEC/RFP) at a 5:1 ratio. Plates were kept for 24 hours in a humidified incubator at 37°C and 5% CO_2 and culture medium was replaced three times a week.

Microfluidic device fabrication and perfusion protocol. The miniaturized, optically accessible microfluidic device used in this study was an improved version of a previously described prototype (3). The flow gasket – comprising flow channels and scaffolds chamber – was made from polydimethylsiloxane (DowCorning), via replica molding. Polycarbonate molds were milled with a computer numerically controlled (CNC) machine. The flow gasket was permanently bonded to a standard glass slide (Fisher Scientific) through air plasma surface activation. To seal the perfusion chamber, glass cover slips (Fisher Scientific) was placed on top of the flow gasket. Each flow gasket had three inlet-outlet channels and three independent chambers, allowing interstitial perfusion. Glass slide, flow gasket and cover slip were kept tightly together using custom made magnetic holders designed to fit a microscope stage and to preserve optical accessibility. The magnetic pieces, with wells that fit cylindrical magnets (6.5 mm diameter, 3.20 mm thick; kjmagnetics), were obtained machining Ultem sheets (6.5 mm thick, 100 mm wide; McMaster). Inlet and outlet channels were connected to stainless steel G15 hypodermic blunt needles (McMaster) and silicone tubing (1.75 mm inner, 3.18 mm outer diameter; McMaster). The outlet tubing was connected to a glass vial that served as waste reservoir, whereas the inlet tubing was connected to disposable syringes (Fisher Scientific). Because air bubbles could form within the perfusion loop during tissue cultivation, we designed a custom-made bubble trap connected to the inlet loop. PDMS cylindrical wells were casted from CNC machined molds. The inlet needle was placed higher than the outlet needle to ensure that air bubbles move upward reaching the highest point in the trap. Flow rates and fluid volumes were controlled using a syringe pump (Harvard Apparatus).

Histology, immunohistochemistry (IHC) and immunofluorescence (IF). Samples were washed in PBS, fixed in 10% (vol/vol) formalin at room temperature for 24 hours, decalcified for 24 hours with Immunocal solution (Decal Chemical Corp.). Constructs were then dehydrated in graded ethanol solutions, paraffin embedded, sectioned to 5 µm thickness. For immunohistochemistry tissue sections were deparaffinized with CitriSolv, and rehydrated with graded series of ethanol washes. Antigens retrieval was performed by incubation in citrate buffer (pH 6) at 90 °C for 15 min, while endogenous peroxidase activity was blocked with H2O2 [3%(vol/vol)]. After washing with PBS, sections were blocked with horse serum and stained with primary antibodies overnight in a humidified environment. The primary antibodies used were anti-CD146 (dilution 1:50; Abcam; ab75769) anti-PDGFR-β (1:25; Santa Cruz; sc-432) and anti-NG2 (1:50; Abcam; ab50009). After washing with PBS, samples were incubated with secondary antibodies for 1h at 25°C and developed (Vector Laboratories). Negative controls were prepared by omitting the primary antibody step. Slides were counterstained with Hematoxylin QS (Vector Labs). Results of histological and immunohistochemical staining were processed using light microscopy with the same illumination, capture time, and white balance settings for all culture groups and negative staining controls. For the immunofluorescent staining, the sections were blocked using 1% BSA in HBSS at room temperature for 1 hour, and incubated with periostin mouse monoclonal antibody (AdipoGen, clone: Stiny-1). A goat anti-mouse Alexa fluor 488 (dilution 1:500; Abcam) was used as the secondary antibody. Samples were counterstained and mounted using Vectashield-DAPI to visualize cells' nuclei. Cell counting was performed as previously described (4). Briefly, individual cells were identified on 5 µm sections taken every 100 µm, by the presence of a nuclear stain (H&E) and cells counts were adjusted using Abercrombie's correction to prevent overrepresentation of cell number. The low-magnification – high-resolution images of histological

sections were obtained by digitizing the tissue sections using the Olympus dotSlide 2.4 digital virtual microscopy system (Olympus, Japan, Tokyo) at a resolution of 0.32 µm. The device captures multiple images at high magnification and stitches them together to form a composite image representing the high-resolution overview of the tissue section.

Tumor Cell Area Fraction from live confocal imaging. Tumor cell area fraction was measured as previously described (11). For GFP expressing breast cancer cells MDA-MB-231, day 7 (24 hours after tumor cell seeding), 10, 17 images were subjected to constant threshold within each experiment to eliminate variability. The total area fraction was then calculated. For each image, the measured area fraction at day 10 and day 14 was normalized by the corresponding day 7 value to account for any variations in seeding density.

Quantitative real-time PCR (qRT-PCR). qRT-PCR was performed as previously described (5). Briefly, total RNA was extracted using Trizol (Thermo-Fisher) following the manufacturer's protocol. To generate cDNA, RNA preparations (2 µg) were treated with "Ready-to-go you-prime first-strand beads" (GE Healthcare). Quantitative real-time PCR was performed using DNA Master SYBR Green I mix (Applied Biosystems). mRNA expression levels were quantified applying the ΔCt method, ΔCt = (Ct of gene of interest - Ct of GAPDH). qRT-PCR primer sequences were obtained from the PrimerBank database (http://pga.mgh.harvard.edu/primerbank/) (Table S3).

Micro-computed tomography. Bone scaffolds were scanned using a Scanco vivaCT 80 system (Scanco Medical AG, Bassersdorf, Switzerland) with energy settings of 55kVp and 145µA, and an integration time of 300ms. Images were reconstructed using standard Scanco software at an isotropic voxel size of 10.4 microns. Grayscale images were subjected to a Gaussian filter (sigma=.8, support=1) to reduce noise and thresholded at 30% of the maximum grayscale value to produce segmented 3D images.

Computational model. A multiphysics computational finite element (FE) model was developed to predict both the fluid dynamics variables, including the average velocity, the hydrodynamic shear stress, and the oxygen concentration within the chip. Three bone CT samples were reconstructed by an image processing software for 3D design and modeling (Mimics, Materialise), exported as solid to layer files (.stl) and then imported in the software Comsol Multiphysics® (Comsol 2015). The culture chamber was 8-mm length, 3-mm width and 1-mm height. Both the inlet and the outlet geometrical parts were designed with a curvature radius of 2 mm. The geometry and the boundary conditions for the computational study are shown in Fig. S3. In the fluid dynamics problem, the experimental flow rates were imposed on the left surface of the modelled culture chamber (inlet), a null pressure at the right surface (outlet). No slip boundary conditions ($\boldsymbol{u} = 0$) were imposed on both the surface of the culture chamber and the bone scaffold. The software Comsol Multiphysics® (Comsol 2015) was used to set up, discretize and solve the equations. The final mesh was composed of 4×10^6 tetrahedral elements. The numerical analyses were run on a Linux workstation with 32 Gb RAM.

Fluid velocity and shear stress in the perfused culture.
The medium fluid dynamics was modelled using the Navier-Stokes equations for incompressible Newtonian fluids, namely by the continuity (Eq.1) and the momentum conservation equation (Eq. 2), respectively:

$$\nabla \cdot u = 0 \quad (1)$$

$$\rho(\boldsymbol{u} \cdot \nabla)\boldsymbol{u} = \nabla \cdot \left(-p\boldsymbol{I} + \mu(\nabla \boldsymbol{u} + (\nabla \boldsymbol{u})^T)\right) + \boldsymbol{F} \quad (2)$$

where $\boldsymbol{u}$ is the velocity vector, ρ is the fluid density, p is the fluid pressure, μ is the dynamic viscosity of the fluid and $\boldsymbol{F}$ is the volume force vector. The hydrodynamic shear stress τ was calculated by Eqs. 3 and 4:

$$\tau = \sqrt{\tau_{12}^2 + \tau_{23}^2 + \tau_{13}^2} \quad (3)$$

$$\tau_{ij} = \mu\left(\frac{\partial u_i}{\partial x_j} + \frac{\partial u_j}{\partial x_i}\right) \quad (4)$$

Oxygen tension and consumption in the perfused culture.
For the mass transport equations, insulation boundary conditions were imposed on both the culture chamber walls and the bone scaffold, under the hypothesis of impermeable walls ($-\boldsymbol{n} \cdot \boldsymbol{J} = 0,$ where $\boldsymbol{J}$ is the flux and $\boldsymbol{n}$ is the normal vector to the surface). A constant inlet concentration c and a condition of convective flux were imposed on the left (inlet) and the right surface (outlet) of the modelled culture chamber, respectively.
The mass transport equation in the fluid domain was modelled as follows (Eq.5):

$$\boldsymbol{u}\boldsymbol{\nabla} \cdot c - D\Delta c = 0 \quad (5)$$

where c is the oxygen concentration, D is the diffusion coefficient of oxygen in the culture medium at 37°C and $\boldsymbol{u}$ is the fluid velocity predicted by Eqs. 1 and 2.
Because cells populated the trabecular space (pores), cell metabolic activity was modeled in the void volume of the porous 3D bone scaffold (Table 1, Fig. S2.) (Eq.6):

$$\boldsymbol{u}\boldsymbol{\nabla} \cdot c - D\Delta c = \tilde{V} \quad (6)$$

where $\tilde{V}$ is the cell volumetric consumption rate that was assumed to be a function of the concentration of oxygen according to the Michaelis–Menten (M-M) kinetics:

$$\tilde{V} = V \cdot \frac{c}{c + K_{MM}} N_V^i \quad (7)$$

V and K_{MM} being the maximal consumption and the M-M constant of for the oxygen (6, 7) and N_V^i (superscript *i* = *e* refers to experimental cell seeding density, superscript *i* = *A* stands for the cell density estimated by the Abercrombie method (8). Briefly, 10 histological images of 3 bone scaffolds for each culture conditions (static and perfused) were analyzed. Images were processed using the deconvolution function in the Imagej software (Imagej,NIH) and nuclei were counted by two operators independently. The cell density for each bone scaffold was calculated as follows:

$$N_V^A = \frac{\bar{N}}{t + d_{Nuclei}} \quad (8)$$

where $\bar{N}$ is the average number of cell per image area (300 × 300 µm), t is thickness of the histological section (5 µm) and d_{Nuclei} is the average nuclear diameter. The parameters imposed in the numerical analyses are summarized in Table 2 and the calibration procedure was performed in a previous study (9).

Micro particle image velocimetry analysis. Fluorescent beads (Polyscience) of 1 µm diameter were used as tracer particles and mixed in culture medium at 2.3 × 10^7 particles ml^{-1}. The motion of the fluorescent beads flowing through the perfusion chamber and the 3D scaffold was observed using a fluorescent microscope (BX-50, Olympus Optical Co. Ltd.) and recorded with a highspeed camera

(Phantom V7.1; Vision Research Inc.) at 500 images s^{-1}. Velocity maps and average velocity profiles were calculated from captured images using the PIV analysis application in MatLab (MathWorks).

Confocal microscopy. Fluorescent images HUVEC/RFP and MDA-MB-231/GFP cells were captured using a Nikon A1 scanning confocal microscope on an Eclipse Ti microscope stand (Nikon Instruments, Melville, NY) using a 10x/0.3 Plan Fluor (Nikon) objective. The confocal pinhole was set at 1 Airy unit, to produce an optical section of approximately 17 µm. GFP was excited at 488 nm and emission was collected from 500-550 nm. RFP was excited at 561 nm and emission was collected from 570-620 nm. Channels were imaged sequentially to prevent bleedthrough. Z series were collected through the depth of the tissue section and maximum projections renderings were generated using NIS Elements software (Nikon). Quantitative analysis of HUVEC/RFP vascular networks was performed using AngioTool as previously described (10).

Drug studies. For drug studies in monolayer, 5 × 10^3 breast cancer cells expressing the firefly luciferase gene (MDA-MB-231/Luc) were plated in a 96-well plate with 200 µL of culture medium. After 24 hours, sunitinib was added to each well at a specified concentration, and luciferase intensity was measured after 3 days of incubation.
For drug studies in the BoPV model, endothelial cells and MSCs were grown statically on the 3D bone matrix for 7 days. Breast cancer cells MDA-MB-231/Luc were added to the co-culture and exposed to fluid flow using the microfluidic chip for 4 days. Then, 3.5 µM of sunitinib were added to the perfusion loop and tissues were treated with the drug for 3 days. Static cultures were cultured in 24-well tissue culture dishes and treated similarly, while controls were exposed to the drug vehicle. To assess cancer cell growth, samples were harvested and processed for the luciferase assay.

Luciferase assay. ONE-Glo™ luciferase substrate was prepared according to manufacturer's protocol (Promega, E6110). Samples were collected and cut in half at previously described time points and placed into 100 µl of media within a 96 well clear bottom black plate (Corning). An equivalent volume of luciferase substrate was mixed in via pipetting, and allowed to incubate in the dark for at least 10 minutes. Following incubation, the samples were measured for luminescence signal using a TECAN Infinite® M200 PRO series microplate reader.

Statistical analysis. Experimental data are presented as mean ± S.D. unless noted otherwise. Statistical tests were performed with an independent Student t test for two groups of data. P value < 0.05 was considered significant.

Supplementary Figures

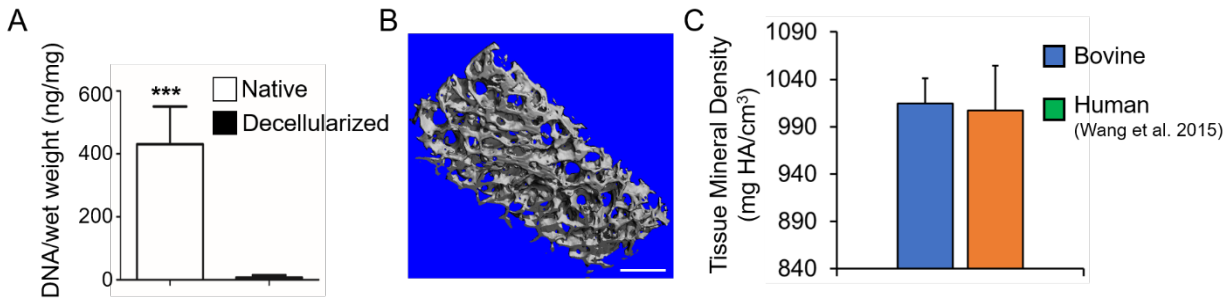

Fig. S1 Bone decellularization and mineral density. (A) Bone tissue DNA content (ng) before (native) and after the decellularization. Values are normalized to the tissue wet weight (mg). **(B)** Reconstructed 3D µCT images of the mineralized bone tissues. **(C)** Tissue mineral density (TMD) measurements expressed in mg of hydroxyapatite per cubic centimeter of bovine trabecular bone (measured in this study) compared to human trabecular bone (measured in (11)). Data in A is represented as average + s.d; n= 3; *** p<0.001, unpaired two-tailed Student t-test.

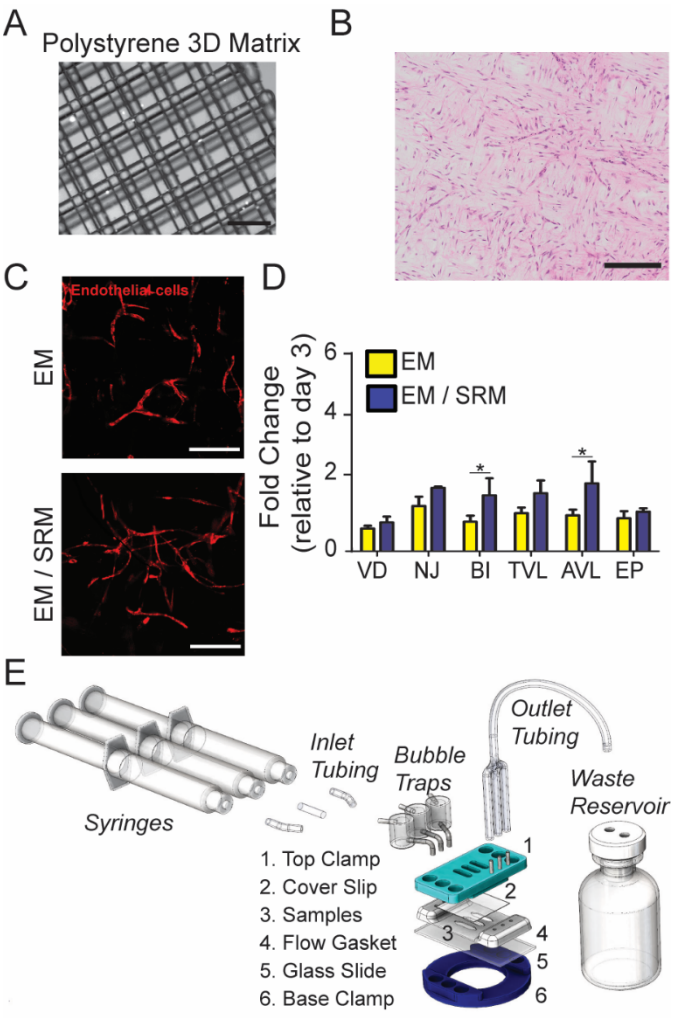

Fig. S2 Vasculogenesis in 3D polystyrene matrix and overview of the microfluidic chip. (A) Phase contrast image of the 3D polystyrene matrix. Scale bar: 100 µm. **(B)** Hematoxylin and Eosin staining of MSCs and ECs co-cultured in the polystyrene 3D matrix in serum reduced medium. Scale bar: 100 µm. **(C)** Confocal images of RPF-labeled ECs forming vascular networks in the 3D polystyrene matrix**.** Scale bars: 200 µm. **(D)** Quantification of neo-vessel formation using confocal images. Vessel density (VD), number of junctions (NJ), branching index (BI), total vessel length (TVL), average vessel length (AVL) and number of endpoints (EP) were measured after 2 weeks of culture and normalized to day 3 values. **(E)** Overview of the microfluidic chip and perfusion loop used to expose the BoPV niches to interstitial flows. Interstitial perfusion was controlled via syringes containing culture medium and connected to a syringe pump. The samples were placed in an optically accessible perfusion chamber assembled using a glass slide (bottom), a PDMS flow gasket (middle) and a glass cover slip (top), allowing for continuous evaluation of tissue development over time. Culture medium was perfused from the inlet tubing connected to bubble traps and inside the perfusion chambers housing the samples. Cellular and metabolic waste was collected in glass bottles placed at the outlet of the flow gasket (waste reservoir).

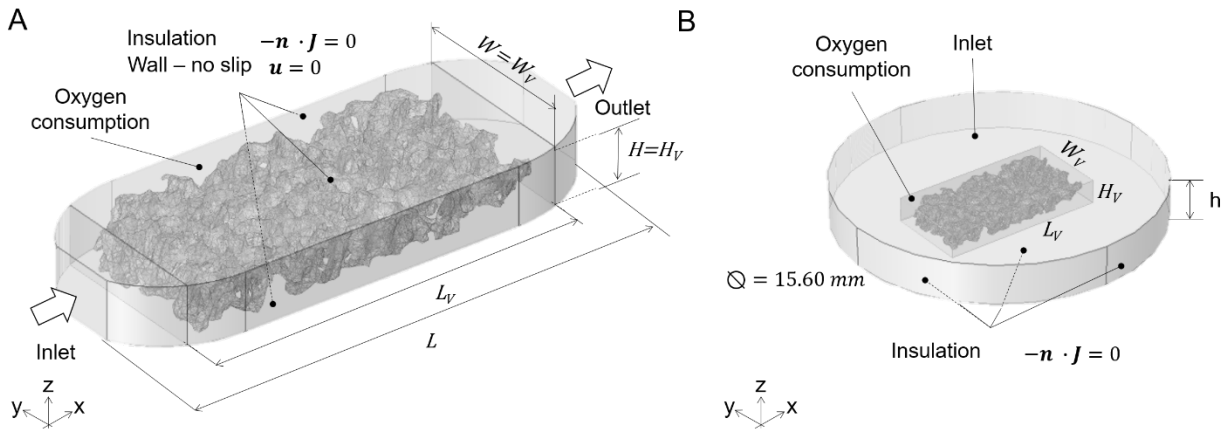

Fig. S3 Computational model geometry and boundary conditions. (A) Isometric view of the perfusion chamber housing the bone scaffold (interstitial flow). **(B)** Isometric view of tissue culture well-plate and the bone scaffold (static culture)**.**

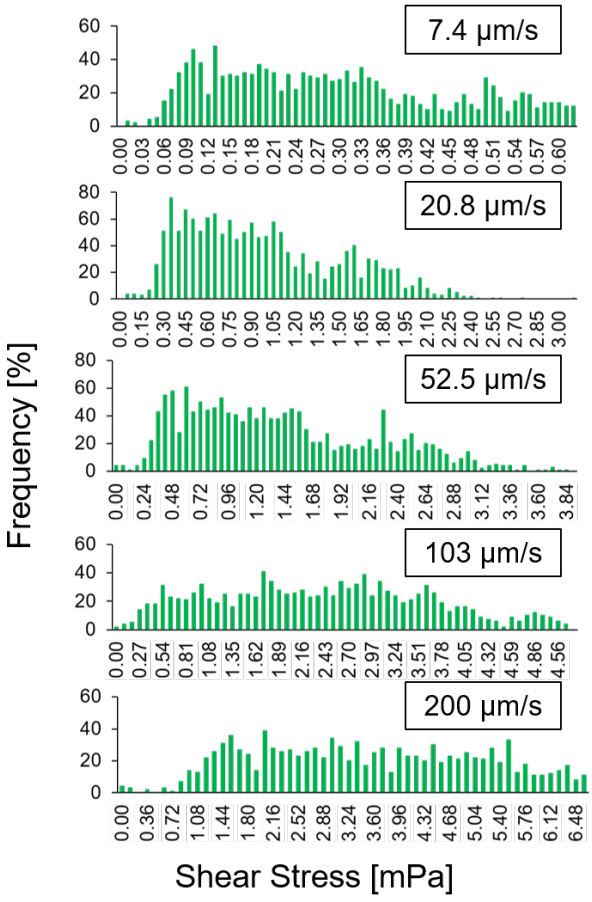

Fig. S4 Shear stress distribution. Histogram representing the shear stresses magnitudes and their frequency arising in the BoPV niche perfused at different flow velocities.

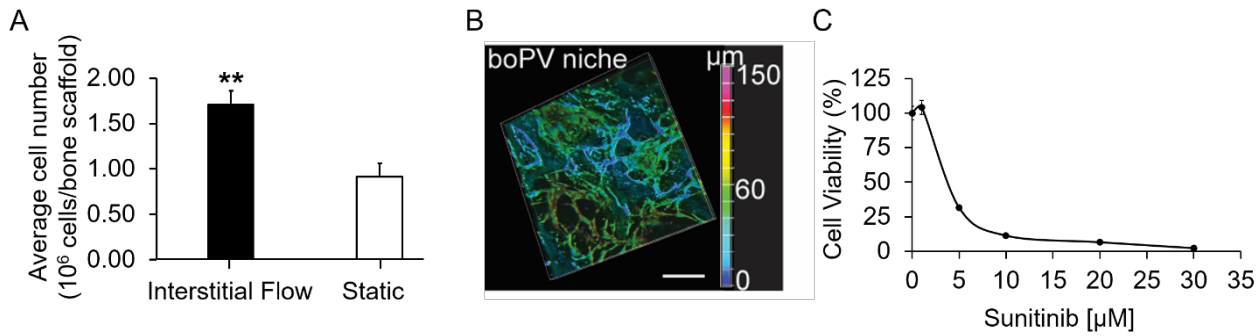

Fig. S5 Cell Number, vascular network and drug sensitivity. (A) Average cell number of the MSCs-ECs populated bone scaffolds exposed to interstitial flow or cultured in static conditions at day 14 (n = 10 images, N=3 samples). **(B)** Confocal reconstruction of flow-induced 3D microvascular network in the BoPV niche; color-coded by depth. Scale bar: 200 µm. **(C)** Breast cancer cells MDA-MB-231/Luc were exposed to increasing concentrations of sunitinib for 48 hours. Luciferase assay was used to measure cancer cells survival. Intensity values were normalized to the luciferase activity cells treated with the vehicle (control). Data is represented as average + s.d; n= 6; ** p<0.01, unpaired two-tailed Student t-test. Cell viability expressed as percentage of non-treated cells.

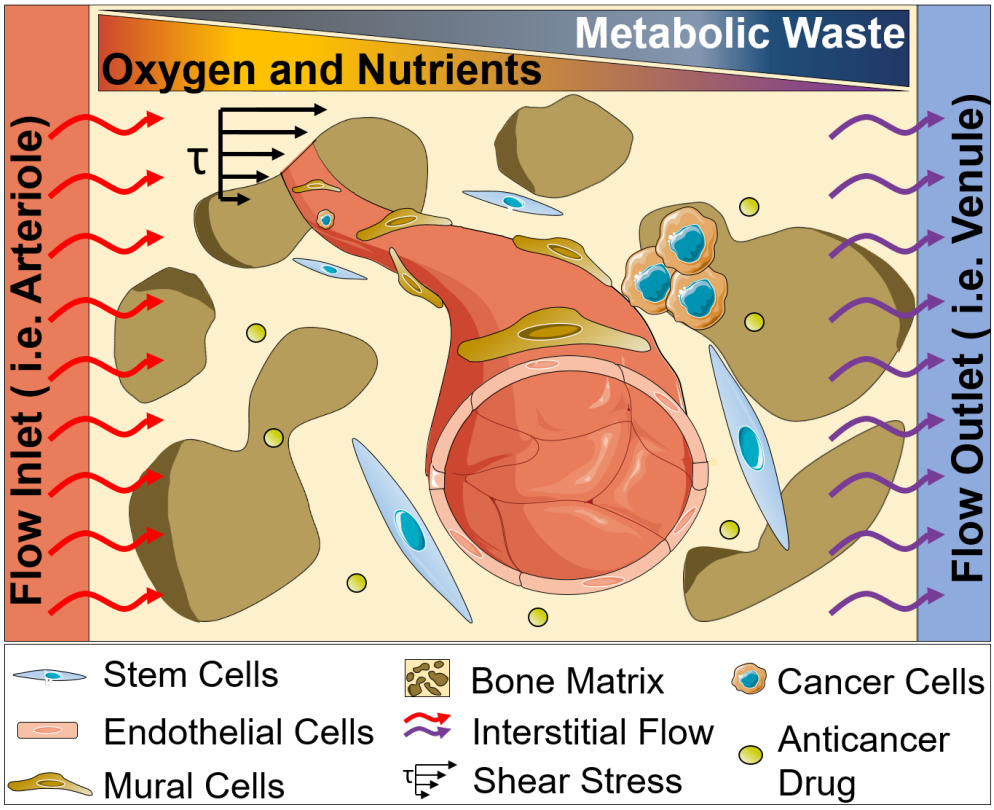

Fig. S6 Schematic representation of the BoPV niche-on-a-chip. Cancer cells home the bone perivascular niche-on-a-chip and adapt to biophysical and biochemical cues driven by flow, extracellular matrix and cells. MSCs, mural cells and ECs that populate the niche, interacted with the homing cancer cells. Anticancer drugs, targeting the proliferating cancer cells, failed to affect slow proliferating cancer cells, which survived in the niche.

Supplementary Tables

Table 1. µCT structural parameters measured from bone scaffolds (n=3).

Values	Average ± SD
Total volume [mm^3]	15.0 ± 1.1
Bone volume [mm^3]	3.3 ± 0.4
Porosity [%]	80.0 ± 4.0
Connectivity density [1/mm^3]	54.1 ± 14.9
Trabecular number [1/mm]	2.9 ± 0.2
Trabecular thickness [mm]	0.1 ± 0.01
Trabecular space [mm]	0.3 ± 0.02

Table 2. Parameters used in the computational multiphysics analyses.

Symbol [units]	Value	Description	Reference
H [mm]	1	Culture chamber height	this study
L [mm]	8	Culture chamber length	this study
W [mm]	3	Culture chamber width	this study
H_V [mm]	1	Scaffold height	this study
L_V [mm]	6	Scaffold length	this study
W_V [mm]	3	Scaffold width	this study
Q_{in} [µl min^{-1}]	0.25 0.50 1.50 2.50 5.00 10.00	Flow rates at the inlet	this study
μ [10^{-4} Pa s]	8.10	Dynamic viscosity of medium at 37° C	(7)
ρ [kg m^{-3}]	1000	Density of medium at 37° C	(7)
D [10^{-5} cm^2 s^{-1}]	3.29	Oxygen diffusion coefficient in medium	(6)
V [µmol 10^{-6} $cells^{-1}$ s^{-1}]	0.0017	Oxygen consumption rate	(6)
K_{MM} [mol cm^{-3}]	1. 10^{-8}	M-M constant for oxygen	(6)
N_V^A [cells mm^{-3}]	1.56-1.86 10^{-6}	Estimated cell density in the porous volume	this study
c [mol m^{-3}]	0.20	Oxygen concentration at the inlet	(6,7)

Table 3. List or primers used for the qRT-PCR.

Gene	PrimerBank ID
HIF1α	194473734c1
POSTN	209863010c2
TGFB1	260655621c1
TGFBR1	195963411c1
TGFBR2	133908633c2
Survivin (BIRC5)	59859879c1
TSP1 (THBS1)	40317625c1
VEGFR2 (KDR)	195546779c1
VEGFR1 (FLT1)	229892219c1

References

1. de Peppo GM, Marcos-Campos I, Kahler DJ, Alsalman D, Shang L, Vunjak-Novakovic G, et al. Engineering bone tissue substitutes from human induced pluripotent stem cells. Proc Natl Acad Sci U S A. 2013;110(21):8680-5.
2. Marturano-Kruik A, Villasante A, Yaeger K, Ambati SR, Chramiec A, Raimondi MT, et al. Biomechanical regulation of drug sensitivity in an engineered model of human tumor. Biomaterials. 2018;150:150-61.
3. Lagana M, Raimondi MT. A miniaturized, optically accessible bioreactor for systematic 3D tissue engineering research. Biomed Microdevices. 2012;14(1):225-34.
4. Betley JN, Cao ZF, Ritola KD, Sternson SM. Parallel, redundant circuit organization for homeostatic control of feeding behavior. Cell. 2013;155(6):1337-50.
5. Villasante A, Marturano-Kruik A, Vunjak-Novakovic G. Bioengineered human tumor within a bone niche. Biomaterials. 2014;35(22):5785-94.
6. Zhao F, Pathi P, Grayson W, Xing Q, Locke BR, Ma T. Effects of oxygen transport on 3-d human mesenchymal stem cell metabolic activity in perfusion and static cultures: experiments and mathematical model. Biotechnol Prog. 2005;21(4):1269-80.
7. Nava MM, Raimondi MT, Pietrabissa R. A multiphysics 3D model of tissue growth under interstitial perfusion in a tissue-engineering bioreactor. Biomech Model Mechanobiol. 2013;12(6):1169-79.
8. Abercrombie M. Estimation of nuclear population from microtome sections. Anat Rec. 1946;94:239-47.
9. Raimondi MT, Giordano C, Pietrabissa R. Oxygen measurement in interstitially perfused cellularized constructs cultured in a miniaturized bioreactor. J Appl Biomater Funct Mater. 2015;13(4):e313-9.
10. Zudaire E, Gambardella L, Kurcz C, Vermeren S. A computational tool for quantitative analysis of vascular networks. PLoS One. 2011;6(11):e27385.
11. Wang J, Kazakia GJ, Zhou B, Shi XT, Guo XE. Distinct Tissue Mineral Density in Plate- and Rod-like Trabeculae of Human Trabecular Bone. J Bone Miner Res. 2015;30(9):1641-50.